Characterization of unreinforced and steel wire reinforced magnesium alloy AZ31 under mechanical-corrosive loading

A. Reeb, L. Schweizer, Kay A. Weidenmann, V. Schulze

Angaben zur Veröffentlichung / Publication details:

Reeb, A., L. Schweizer, Kay A. Weidenmann, and V. Schulze. 2014. "Characterization of unreinforced and steel wire reinforced magnesium alloy AZ31 under mechanical-corrosive loading." *Procedia CIRP* 18: 114–19. https://doi.org/10.1016/j.procir.2014.06.117.

Available online at www.sciencedirect.com

ScienceDirect

Procedia CIRP 18 (2014) 114 – 119

www.elsevier.com/locate/procedia

International Conference on Manufacture of Lightweight Components – ManuLight2014

Characterization of unreinforced and steel wire reinforced magnesium alloy AZ31 under mechanical-corrosive loading

A. Reeb*, L. Schweizer, K.A.Weidenmann, V. Schulze

Institute of Applied Materials, Karlsruhe Institute of Technology, Germany

* Corresponding author. Tel.: +49 (0) 721 608 47441; fax: +49 (0) 721 608 48044; *E-mail address*: andreas.reeb@kit.edu

Abstract

In this work, the sensitivity of an unreinforced and steel wire reinforced AZ31 magnesium alloy to stress corrosion cracking is investigated by means of static stress corrosion testing (clamping lever tests) and cyclic stress corrosion testing (crack propagation tests). In static mechanical-corrosive testing, the AZ31 alloy showed a relatively low sensitivity while the composite showed a higher sensitivity with earlier crack initiation due to weakening of the loaded specimen section. In cyclic experiments, hydrogen embrittlement crack growth acceleration could be attested. Reinforcing the matrix material leads to a compensation of the crack growth acceleration due to stress corrosion cracking by crack energy absorption by increased interface damage according to the aggressiveness of the corrosive media.

Peer-review under responsibility of the International Scientific Committee of the "International Conference on Manufacture of Lightweight Components – ManuLight 2014"

Keywords: stress corrosion cracking, cylic loading, 301SS, clamping lever test, crack propagation, interface corrosion

1. Introduction

By development of new metal matrix composites the specific properties, like specific strength or stiffness, can be increased above the level of conventional light metal alloys, which leads to an improved lightweight construction performance. The composite extrusion process represents one strategy for producing unidirectional reinforced light metal matrix composites [1]. Profiles manufactured by composite extrusion are suited perfectly for light frame structures in vehicle construction and aviation. The stresses occurring in this field of application are mostly of cyclic nature and are often superimposed by corrosive exposure. Additionally, static stress corrosion cracking (static SCC) and especially cyclic stress corrosion cracking (cyclic SCC) are critical damage mechanisms for the application of magnesium alloys [2, 3]. These mechanisms may be of even higher relevance when using magnesium alloys in metal matrix composites.

For this reason the influence of mechanical and superimposed corrosive conditions in a steel wire-magnesium matrix composite shall be investigated qualitatively in this work by means of static exposure tests and cyclic crack propagation tests.

In general, magnesium alloys are considered to be relatively sensitive to corrosion in liquid solutions, where the corrosion process is mostly dominated by hydrogen corrosion according to [4]:

$$2Mg + 2H^+ + 2H_2O \rightarrow 2Mg^{2+} + 2OH^- + 2H_2 \qquad (1)$$

But most important for magnesium matrix composite is the circumstance of a high negative free corrosion potential of -1,7 V in watery solutions, which leads to a preferential active corrosion of magnesium in contact with other metals or other phases leading to selective corrosion mechanisms like pitting [4].

It is already known that embedded reinforcing elements in metal matrix composites can lead to a crack deceleration by interaction between crack tip and interface [5, 6]. However, in corrosive conditions an increased interfacial damage is expected and therefore the crack tip – interface interaction can be influenced strongly, as shown for an aluminum matrix composite in [7].

Peer-review under responsibility of the International Scientific Committee of the "International Conference on Manufacture of Lightweight Components – ManuLight 2014"
doi:10.1016/j.procir.2014.06.117

2. Experimental Work

2.1. Materials

The magnesium composite used in this study is an AZ31 (MgAl3Zn) magnesium alloy reinforced with a spring steel wire 301SS (X10CrNi18-8) with a diameter of 1 mm. The investigated 40x10 mm² rectangular profiles were manufactured on a 10 MN extrusion press with a press ratio of 42:1 at a ram speed of 0.5 mm/s [1]. The billet temperature was set to 360 °C.

Table 1 gives an overview of the chemical composition of the AZ31 matrix alloy and the 301SS reinforcement elements measured by spectral analysis. It has to be noted that the Al-content is slightly below the range of tolerance given by DIN 1729-1 [8] and the Ni-content is clearly above the allowed level of 0,005 wt-%.

Table 1 Measured chemical analysis of AZ31 and 301SS in wt-%

AZ31	**Al**	**Zn**	**Mn**	**Si**
	2,48	0,99	0,38	0,02
	Fe	**Cu**	**Ni**	**Rest**
	0,013	-	0,012	0,127
301 SS	**C**	**Si**	**Mn**	**P**
	0,07	0,52	0,93	0,03
	N	**Cr**	**Mo**	**Ni**
	0,04	18,2	0,43	8,3

2.2. Specimen geometry

The investigations regarding the static stress corrosion sensitive were done by a clamping lever test according to DIN 7539-2 [9]. The specimen geometry is shown in figure 1.

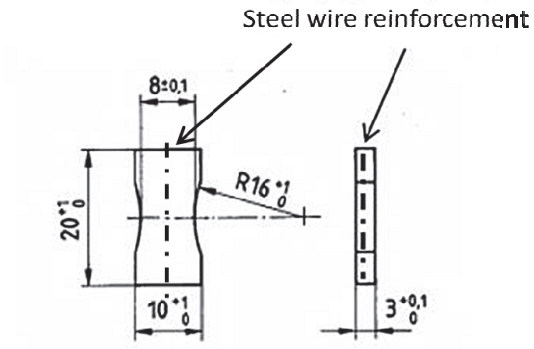

Fig.1. Specimen geometry for the clamping lever tests [9]

The reinforcing element is positioned in the center of the specimen with a displacement from the neutral axis of 0.5 mm towards the outer edge. The reinforcement ratio in the smallest cross section (= tested cross section) of the specimen was 3.27 vol-%.

Figure 2 shows the notched M(T)-specimen geometry used according to ASTM E 647 [10]. The cross-section of the specimen is equal with the cross-section of the net-shape manufactured profile. The reinforced profiles were reinforced with five steel wires. The center reinforcing element is cut during specimen processing, which leads to an effective reinforcement ratio of 1.065 vol- % in the resulting specimen.

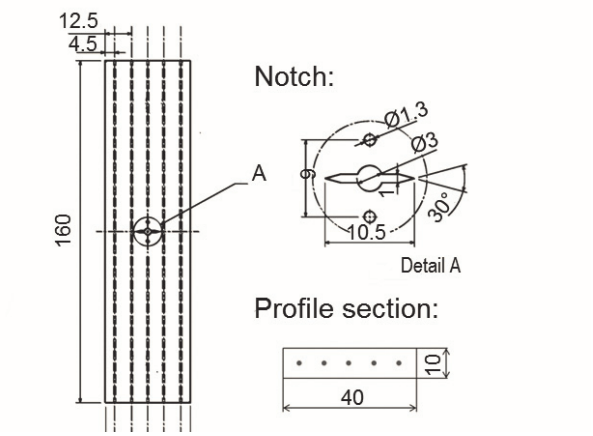

Fig.2. M(T) specimen geometry for cyclic crack growth experiments according to [10]

2.3. Setup

The experimental setup for the clamping lever test is shown in Figure 3. The load F_V was applied with two aligned steel points in a universal testing machine type Zwick I under load control, resulting in an outer fiber stress of 75 % $R_{p0.2}$ of the matrix material.

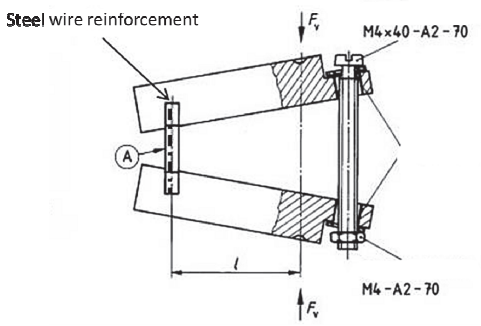

Fig. 3. Setup for the clamping lever test [9]

For corrosive exposure the clamped specimens are put into the corrosive medium in plastic basins afterwards. By using a dyadic setup with an inner and outer basin, a uniform flow and circulation of the corrosion media was ensured by an air supply at the bottom of the outer basin (Figure 4).

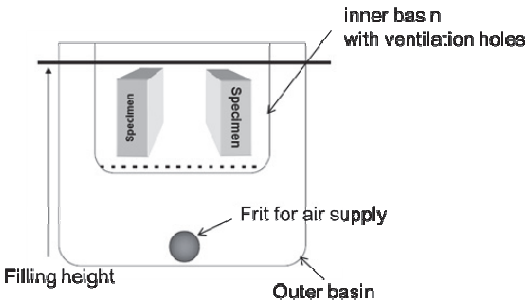

Fig. 4. Testing setup for exposure with corrosive media

The unreinforced and reinforced clamping lever samples, as well as unloaded reference samples, were exposed for a maximum of 30 days. The surface crack initiation and surface corrosion was surveyed by examining the specimens in regular intervals using light microscopy.

The cyclic experiments were performed in tension at R = 0.18 on a vibraphore testing system of type Amsler ±HFP 5000, which has a maximum test load of 50 kN. Prior to the experiment a crack was initiated with a medium load of F_m = 7 kN and an amplitude of F_a = 5 kN, up to an initial crack length of about 9.7 mm for consistent original conditions. The subsequent experiment was carried out at F_m = 5.5 kN, F_a = 3.8 kN and R = 0.18.

Reference experiments were performed in laboratory atmosphere and for corrosive superimposing at cyclic and static loading, with corrosive media representing the most common application cases. Besides distilled water as liquid reference medium, a 3.5 wt-% sodium chloride solution for representing sea water or an exposure to road salt and water in typical winter conditions and an acid sulfur solution with pH = 5 as replacement for acidic rain were chosen. The exposure of the crack was realized by a set-up shown in figure 5. The specimen was fixed to the testing machine with a clamp gripping and the plastic corrosion chamber was mounted onto the specimen to allow a constant application of the corrosive medium onto the crack through two symmetrical inlets.

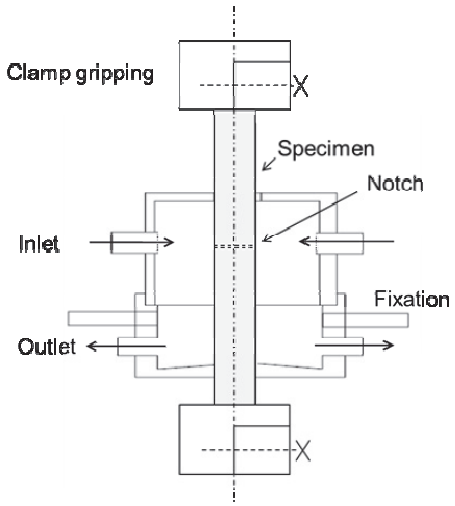

Fig.5. Setup for mechanical corrosive loading for mounting in the vibraphore testing system.

2.4. Crack length measurement in cyclic experiments

While the crack length measurement in laboratory air could be realized simply by potential probe measurement, a stiffness-based crack length determination was developed in previous work [7]. For this purpose, the frequency dependence of the specimen stiffness when using a vibraphore system was exploited. The relationship of frequency f, stiffness c and the excitation mass m of the test machine are shown in equation 2.

$$f = \frac{1}{2\pi}\sqrt{\frac{c}{m}} \qquad (2)$$

$$2a = k + l \cdot \Delta f^{m} \qquad (3)$$

Analogous to the calibration of the potential probe, a calibration curve was determined for the relationship between frequency drop and crack length (Equation 3). The determined parameters were k = -2.9 × 10 -2, l = 53.47, and m = 0.527.

3. Results and discussion

3.1. Clamping lever test

The corrosion damage in all investigated specimen is characterized at the beginning by a linear corrosion of the surface. It can be concluded that in distilled water and sulfur acid solution the corrosion is of selective nature as a linear corrosion pattern according to the extrusion direction is getting visible. In the sodium chloride solution, pitting corrosion was the main damage

mechanism. The unloaded and unreinforced reference samples showed relatively small damage in all cases, whereas the reinforced specimens showed dramatically higher corrosion damage with a quick dissolution of the Mg-matrix beginning from the endings of the specimen where steel wire and matrix are exposed to the electrolyte. In the sodium chloride solution the strongest reaction was observed with a complete uncovering of the steel wire within 6 days (figure 6 d). In distilled water and sulfur acid solution only small damages at the interface were detected.

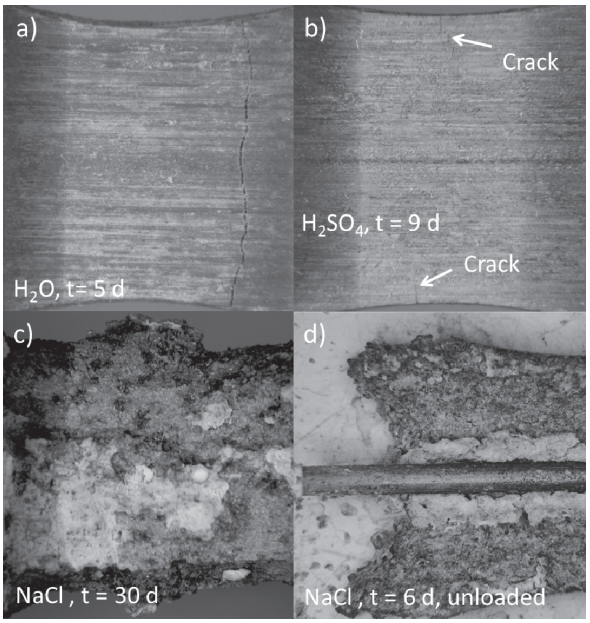

Fig. 6. Surface corrosion and crack initiation in reinforced specimens at time of first crack observation (a,b) or maximum exposure time (c,d).

Under static mechanical loading, crack initiation could be observed in unreinforced specimens only in distilled water during the investigated time frame after about 29 days. In sulfur acid solution and sodium chloride solution the surface corrosion was dominated by pitting damage, while the corrosive attack was much more pronounced as in the unloaded reference specimen. Figure 7 shows the measured time to crack initiation in the loaded specimens. The reinforced specimens interestingly showed a much higher sensitivity to static SCC. In distilled water time until crack initiation was reduced to about 9 days. In the sulfur acid solution cracks could be detected after 5 days. This was not expected as the steel wire-matrix interface was not exposed to the corrosive media. The faster cracking of the composite specimens could be explained by poor interface properties and interface defects resulting in a weakening of the loaded specimen section. In sodium chloride solution, no cracks could be observed, but because of a strong accumulation of corrosion products crack investigations were difficult and initiated cracks could be missed or filled up with corrosion products.

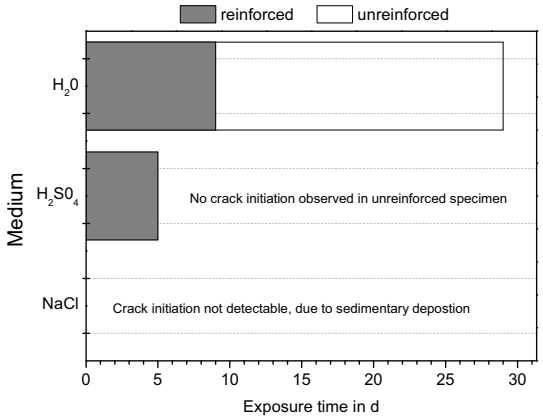

Fig. 7. Exposure time to observation of first crack initiation in unreinforced and reinforced clamping lever specimens.

3.2. Cyclic Crack Growth

Figure 8 shows the measured crack propagation rates in the unreinforced specimen.

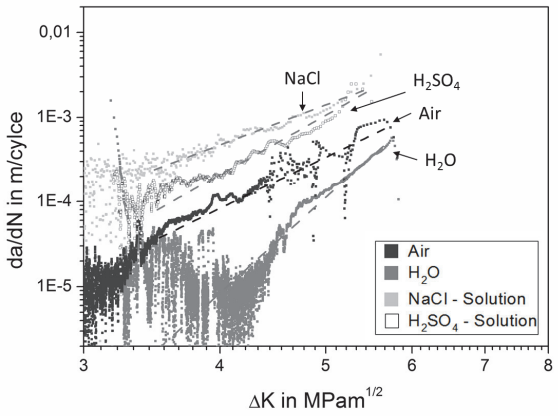

Fig. 8. Crack propagation diagrams for unreinforced specimens.

The influence of the corrosive medium is reflected in a significantly accelerated crack growth. The crack propagation lines are shifted to higher crack propagation rates, thus leading to a reduced specimen lifetime.

In the pure matrix material, the crack propagation rate is largest when exposed with sodium chloride solution followed by the sulfur acid solution. However, the specimens exposed to distilled water showed a shift to lower crack propagation rates compared to the tested specimen in ambient air.

Regarding the SEM-Investigations of the crack surface, it is clearly visible that in distilled water the crack propagation seems to be more fissured. The influence of distilled water seems to provoke this irregular crack growth, as this effect was reproducible in distilled water only.

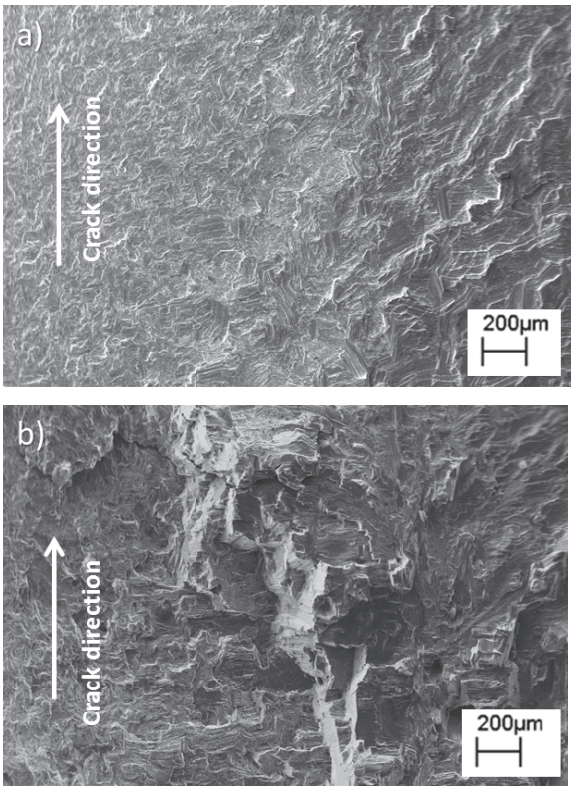

Fig.9. Crack Surface after testing in (a) ambient air (b) distilled water

The fracture surface showed only small amounts of corrosion products (NaCl-solution) or no corrosion products at all (H_2O, H_2SO_4-solution), which indicates a hydrogen embrittlement crack growth acceleration according to [2, 11].

Figure 10 shows the crack propagation diagrams for the reinforced specimens. Here it was detected that the fastest crack growth rates appear in the acid solution followed by distilled water and sodium chloride solution. It has to be noted that the overall crack growth rates do not differ much regarding the different corrosive media.

The region where considerable crack growth acceleration occurs (ΔK = 4.3 – 5) is followed by a deceleration, which could be led back to the interaction of the crack tip with the outer reinforcing elements.

The crack propagation in distilled water is in contrast to the unreinforced specimens characterized by a smooth crack surface, which leads to the assumption that the reinforcement leads to a stabilization of the crack plane.

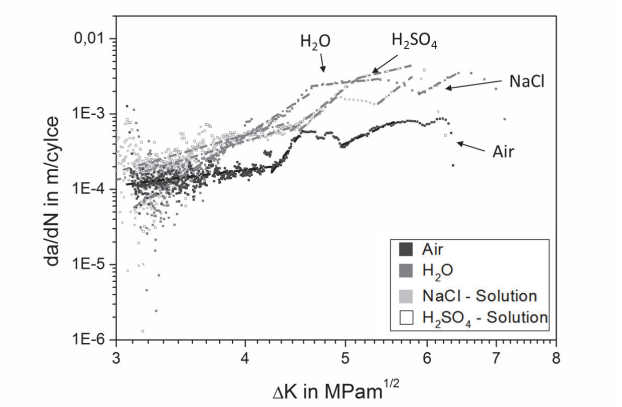

Fig. 10. Crack propagation diagrams for reinforced specimen

It has to be noted that in the composite the crack growth rates lay above those of the unreinforced matrix materials, which was led back to a poor bonding in a low debonding shear strength σ_{deb} of 32.3 MPa (measured by push-out tests) compared to [6]. Figure 11 shows metallographic sections of the crack tip interaction with the reinforcing element in the different corrosive media after cyclic testing. It is visible that the interface degradation is weakest when tested in ambient air.

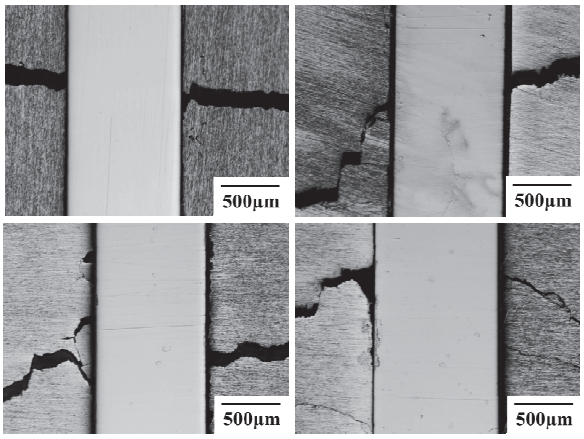

Fig.11. Crack tip / Interface – Interaction in (a) Air (b) H_2O (c) H_2SO_4 solution (d) NaCl-solution

It is worth mentioning that the measurement of the delamination has to be regarded critically as the preparation of the sections is difficult due to different abrasion rates of steel and Mg, which lead to an artificially induced gap at the interface making it hard to distinguish real delamination caused by corrosion and crack propagation along the interface. The degradation of the interface measured by corrosive damage and initiation of multiple side cracks is increased qualitatively in the following order: distilled water,

sulfur acid solution and the highest damage in sodium chloride solution which correlates with the exposure and clamping lever tests.

If it is assumed that the SCC-assisted crack acceleration (shift to higher crack growth rates depending on corrosive medium) in the composite matrix material is the same as in the matrix material, this means that by the reinforcing of the profile, a compensation of this SCC-assisted acceleration is reached according to the corrosive damage which depends on the corrosive medium leading to a similar crack growth rates in all media. As stated in [6], the crack tip interaction with the reinforcing element is characterized by a crack growth along the interface and can lead to an energy absorption eventually resulting in a crack growth deceleration which can be correlated to the damage on the interface. Regarding the shown crack propagation diagrams and the metallographic investigations it is plausible that according to the corrosive influence (highest in sodium chloride solution, lowest in distilled water) the energy absorption is correlated to the interface damage caused by the corrosive media. This leads to an apparent compensation of the particular stress corrosion cracking sensitivity.

4. Summary and Conclusion

In the following, the main results and conclusions are summarized:

- The damage mechanisms in static corrosion application are dominated by selective surface corrosion mechanisms due to an inhomogeneous microstructure typical for magnesium alloys [4].
- If the specimen is reinforced with a steel wire, the negative corrosion potential of magnesium leads to a quick anodic dissolution of the matrix material under exposure of sodium chloride solution if the interface is exposed to the environment. Therefore exposure of the steel wire-matrix interface to maritime environments has to be avoided.
- In cyclic experiments, the reinforcement showed a negative influence in contrast to experiments in [5, 6, 7]. This was lead back to a poor interface bonding and therefore weakening of the composite.
- In corrosive media, the AZ31 alloy showed a significant sensitivity to cyclic stress corrosion cracking suppositionally by a hydrogen embrittlement type crack growth. The composite system could reduce the influence of stress corrosion cracking through reduction of crack growth energy at the interface by increased damage according to the aggressiveness of the corrosive media.

It has been shown that the application of AZ31 as matrix alloy is critical under corrosive loading. Nevertheless, the reinforcing of this alloy with a steel wire can be beneficial in different corrosive environments for fatigue crack growth as the crack growth acceleration remains almost constant in all media. However, for future applications the interface strength has to be optimized to reduce the crack growth rates in the composite system in order to justify the application of such in comparison to the unreinforced material. Yet, the problem of stress corrosion cracking and contact corrosion effects will be inevitable, but as shown in this work, the use of reinforced profiles leads to similar crack growth rates in all media which can result in a more accurate estimation of SCC-assisted crack growth.

Acknowledgements

This paper is based on investigations of the subproject A3 - “Material systems for reinforced and functional extruded profiles” - of the Transregional Collaborative Research Center/Transregio 10, which is kindly supported by the German Research Foundation (DFG).

References

[1] Kleiner, M., Schomäcker, M., Schikorra, M. Klaus, A., 2004. Herstellung verbundverstärkter Aluminiumprofile für ultraleichte Tragwerke durch Strangpressen.Mat.-wiss. u. Werkstofftechn., WILEY-VCH, Weinheim, 35 [7], pp.431-439

[2] R.G. Song, C. Balwert, W. Dietzel, A. Atrens: A study on stress corrosion cracking and hydrogen embrittlement of AZ31 magnesium alloy, MSE-A, 399, 2005

[3] Z. Nan, S. Ishihara, T. Goshima: Corrosion fatigue behavior of extruded magnesium alloy AZ31 in sodium chloride solution, International Journal of Fatigue, 30, 2007

[4] E. Ghali: Corrosion Resistance of Aluminium and Magnesium Alloys, Understanding, Performance and Testing, Wiley INC, New Jersey, 2010

[5] Merzkirch, M. , Weidenmann, K.A., Schulze, V.: Investigations on the Cyclic Crack Growth Behaviour of Spring Steel Wire Reinforced EN AW-6082

[6] M. Merzkirch, V. Schulze, K.A. Weidenmann: Lifetime behavior of unidirectionally wire reinforced lightweight metal matrix composites, Int. J. of Fat. , 56, 2013

[7] A. Reeb, M. Gottschalk, K.A. Weidenmann, V. Schulze: Rissausbreitungsverhalten von federstahldrahtverstärktem EN AW-6082 unter mechanisch-korrosiver Beanspruchung, Verbundwerkstoffe, 19. Symposium Verbundwerkstoffe und Werkstoffverbunde, Her.: A. Wanner u. K.A. Weidenmann, Karlsruhe, 2013

[8] DIN EN ISO 7539-2: Prüfung der Spannungsrißkorrosion. Teil 2: Vorbereitung und Anwendung von Biegeproben Deutsches Institut für Normung, 1995

[9] DIN EN ISO 1729-1Magnesiumlegierungen: Knetlegierungen Deutsches Institut für Normung, 1982

[10] ASTM E 647-05: Standard Test Method for Measurement of Fatigue Crack Growth Rates. ASTM International. 2005

[11] S.P. Lynch: Mechanistics and fractographic aspects of stress-corrosion cracking (SCC), Corros. Rev 30, 2012